Methyl Salicylate Is a Critical Mobile Signal for Plant Systemic Acquired Resistance

Sang-Wook Park, *et al.*

Science **318**, 113 (2007);
DOI: 10.1126/science.1147113

Methyl Salicylate Is a Critical Mobile Signal for Plant Systemic Acquired Resistance

Sang-Wook Park, Evans Kaimoyo, Dhirendra Kumar,* Stephen Mosher,† Daniel F. Klessig‡

In plants, the mobile signal for systemic acquired resistance (SAR), an organism-wide state of enhanced defense to subsequent infections, has been elusive. By stimulating immune responses in mosaic tobacco plants created by grafting different genetic backgrounds, we showed that the methyl salicylate (MeSA) esterase activity of salicylic acid–binding protein 2 (SABP2), which converts MeSA into salicylic acid (SA), is required for SAR signal perception in systemic tissue, the tissue that does not receive the primary (initial) infection. Moreover, in plants expressing mutant SABP2 with unregulated MeSA esterase activity in SAR signal–generating, primary infected leaves, SAR was compromised and the associated increase in MeSA levels was suppressed in primary infected leaves, their phloem exudates, and systemic leaves. SAR was also blocked when SA methyl transferase (which converts SA to MeSA) was silenced in primary infected leaves, and MeSA treatment of lower leaves induced SAR in upper untreated leaves. Therefore, we conclude that MeSA is a SAR signal in tobacco.

Plants respond to pathogen attack by activating both local and systemic defenses that restrict pathogen growth and spread. In the infected leaf, these defenses often involve a hypersensitive response in which necrotic lesions form at the infection site(s) (*1*); the uninoculated tissues subsequently develop systemic acquired resistance (SAR), a state of heightened defense throughout the plant. SAR is similar to acquired immunity in animals in that it is systemic and long-lasting; it also resembles innate immunity, as it provides broad-spectrum resistance to secondary infection (*1*, *2*).

SAR requires movement through the phloem of a signal from the infected tissue to the systemic tissue (leaves above the primary infected leaves) (*3*). Initially, salicylic acid (SA) was postulated to be this mobile signal because it induces defense responses when applied to plants, moves systemically, is found in phloem exudates of infected leaves, and is required in systemic tissue for SAR (*1*, *2*). However, grafting studies showed that infected, SA-deficient rootstocks could trigger SAR in wild-type scions; such results imply that SA is not a mobile SAR signal (*4*, *5*).

To clarify the role of SA in defense signaling, we identified putative SA-effector proteins in tobacco (*6*–*9*). One of these, SA-binding protein 2 (SABP2), is integral to plant innate immunity, as silencing of *SABP2* suppresses both local resistance to tobacco mosaic virus (TMV) and SAR development (*9*). SABP2 is an esterase in the α/β-fold hydrolase superfamily, with strong preference for methyl salicylate (MeSA). It binds SA with high affinity (dissociation constant K_d = 90 nM), resulting in inhibition of MeSA esterase activity (*10*). This suggests that SABP2 functions by converting biologically inactive MeSA (*11*) [which is synthesized from SA by an SA methyl transferase (SAMT) (*12*)] to active SA; feedback inhibition by SA may modulate this process.

To determine whether SABP2 is involved in generating and transmitting the SAR signal in leaves receiving the primary infection and/or perceiving and responding to it in systemic tissue, we performed grafting studies with wild-type (empty vector control) or *SABP2*-silenced rootstocks and scions (*13*) (Fig. 1A). These experiments are informative only if the signal for gene silencing in *SABP2*-silenced tissue is not graft-transmissible to wild-type tissue; this is demonstrated in Fig. 1B. After TMV inoculation, SAR was observed in wild-type scions grafted onto *SABP2*-silenced or wild-type rootstocks. SAR is manifested as a reduction in the size of lesions formed after secondary TMV infection of systemic leaves (scion leaves of grafted plants) on plants that have received a primary infection (on rootstock leaves of grafted plants), relative to the size of lesions developed by plants that previously received a mock inoculation as the primary infection (Fig. 1, C and D). The reduction in lesion size occurs because SAR elicited by the primary infection enables the plant to restrict viral replication and spread more efficiently the second time it encounters the virus. Conversely, plants containing *SABP2*-silenced scions grafted onto wild-type or *SABP2*-silenced rootstocks failed to develop SAR after TMV infection of the rootstock, as evidenced by large secondary lesions formed regardless of whether the rootstock received a primary TMV infection (Fig. 1, C and D). Suppression of SAR in *SABP2*-silenced scions was accompanied by increased viral replication in systemic tissue (Fig. 1D, lower panel) and reduced expression of the *pathogenesis-related 1* gene, which is associated with SAR development (Fig. 1E). These results indicate that SABP2 is required for SAR in

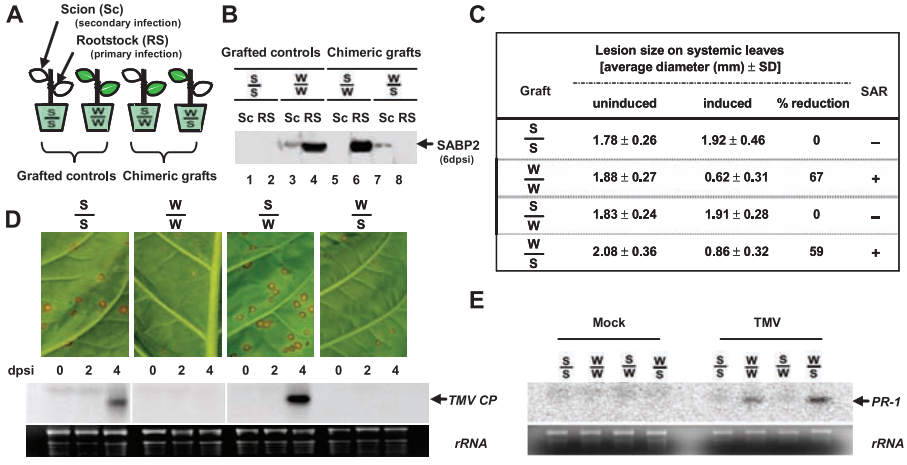

Fig. 1. SABP2 is required for SAR in systemic but not primary infected tobacco leaves. (**A**) Schematic of grafting experiments using wild-type [W; control line C3# expressing an empty vector in *Nicotiana tabacum* cv. Xanthi nc (NN) (*9*)] and *SABP2*-silenced [S; line 1-2# (*9*)] rootstocks (RS) and scions (Sc). (**B**) Immunoblot analysis of SABP2 accumulation in rootstocks and scions of grafted plants (*13*). Nine-week-old plants received a secondary inoculation with TMV at 7 days post primary infection (dppi); SABP2 accumulation was determined at 6 days post secondary infection (dpsi). Note that SABP2 levels are weaker in secondary infected systemic scions at 6 dpsi than in primary infected rootstocks at 13 dppi in controls as well as chimeric grafts. (**C**) Determination of lesion size on scions whose rootstocks received either a mock (uninduced) or TMV (induced) inoculation 7 days before a secondary infection with TMV; lesion sizes were determined at 6 dpsi. (**D**) Upper panel: TMV-induced lesions on scion leaves of the above-described plants at 6 dpsi. Lower panel: RNA blot analysis of TMV *coat protein* (*CP*) transcripts in scion leaves at various times after secondary infection. (**E**) RNA blot of *pathogenesis-related-1* (*PR-1*) expression at 7 dppi (before secondary infection) in grafted scion leaves. Ribosomal RNA (rRNA) is shown as a loading control in (D) and (E).

Boyce Thompson Institute for Plant Research, Tower Road, Ithaca, NY 14853, USA.

*Present address: Department of Biological Sciences, East Tennessee State University, Johnson City, TN 37614, USA. †Present address: Department of Cell and Systems Biology, University of Toronto, Toronto, Ontario M5S 3B2, Canada. ‡To whom correspondence should be addressed. E-mail: dfk8@cornell.edu

systemic tissue, but not for production of a SAR signal in primary infected tissue.

Mutant SABP2 proteins were constructed on the basis of SABP2's three-dimensional structure and produced in *Escherichia coli*; the recombinant proteins were assayed for MeSA esterase activity, SA-binding activity, and SA-feedback inhibition in vitro (table S1). Three mutants were then tested for complementation of SAR in *SABP2*-silenced tobacco: Ala^{13} → Leu (A13L), which lacks SA-binding activity and SA-feedback inhibition; Ser^{81} → Ala (S81A), which lacks MeSA esterase activity; and His^{238} → Ala (H238A), which lacks SA-binding and MeSA esterase activities (Fig. 2A). To prevent RNA interference–mediated silencing of the wild-type or mutant *SABP2* transgenes, we introduced the above mutations into synthetic versions of *SABP2*, *syn1* [formerly *syn* (*14*)] and *syn2*, which share 77% and 60% identity with the native *SABP2* gene, respectively, and are controlled by the estradiol-inducible XVE system (*15*). *syn1* is effectively expressed in *SABP2*-silenced tobacco and restores SAR (*14*). Estradiol treatment of systemic leaves of *SABP2*-silenced plants stably transformed with a *syn* transgene resulted in local synthesis of wild-type or mutant syn SABP2; expression of wild-type *syn1* or *syn2* led to a ~55 to 65% reduction in secondary lesion size, demonstrating that SAR was restored (Fig. 2, B to D). Induction of the A13L mutant in systemic leaves also restored SAR, whereas induction of S81A or H238A did not (these plants had similarly sized primary and secondary lesions and high levels of TMV *coat protein* transcripts in secondary inoculated systemic leaves; Fig. 2, C and D). Thus, SAR requires SABP2's esterase activity, but not its SA-binding activity and SA-feedback inhibition, in systemic leaves.

Although SABP2 is not required in primary infected tissue to generate a mobile SAR signal (Fig. 1 and Fig. 3, A to C), grafted plants containing a wild-type scion and an *SABP2*-silenced rootstock expressing the A13L mutant were SAR-deficient (Fig. 3, A to C). Because the MeSA esterase activity of A13L is not inhibited by SA, whereas that of wild-type SABP2 is, this finding suggests that in wild-type plants, SA-mediated inhibition of SABP2 in the primary infected leaves is critical to allow sufficient MeSA accumulation for SAR induction (Fig. 3D).

Our data argue that MeSA is a mobile SAR signal because SAR requires (i) SABP2's MeSA esterase activity in systemic tissue and (ii) SA-mediated inhibition of this activity in primary infected leaves. This conclusion is supported by gas chromatography–mass spectrometry analyses, which revealed increased MeSA levels in primary infected and, subsequently, systemic leaves of wild-type plants [peaking at 48 and 72 hours post primary infection (hppi), respectively] but not in *SABP2*-silenced plants expressing the A13L mutant in primary infected leaves (Fig. 3D). MeSA levels also increased in phloem (petiole) exudates of primary infected leaves from wild-type plants, peaking at 48 hppi, whereas little increase occurred in plants expressing the A13L mutant (Fig. 3E). In addition, biologically active SA, with or without its biologically inactive conjugated glucoside (SAG), rose in systemic leaves of wild-type plants, whereas little to no rise occurred in SAR-deficient *SABP2*-silenced plants expressing the A13L mutant in primary infected leaves or in *SABP2*-silenced plants (Fig. 3, F and G). Note that the similarity of SA (or SA plus SAG) levels in primary infected leaves of wild-type and *SABP2*-silenced plants expressing A13L (Fig. 3, F and G) was expected because the MeSA level is only 10 to 20% of the SA plus SAG level (Fig. 3, D, F, and G) (*11*); thus, A13L-mediated conversion of most or all of the MeSA to SA would increase SA levels only slightly. Accumulation of SA (or SA plus SAG) in primary leaves of *SABP2*-silenced plants was reduced relative to that in wild-type plants at early times but eventually reached wild-type levels.

In a complementary approach, MeSA levels were reduced by suppressing MeSA biosynthesis via silencing of *NtSAMT1* (fig. S1). Grafting experiments indicate that NtSAMT1 is required in the SAR-signal generating, TMV-infected rootstock, but not in the systemic tissue (i.e., scion) (Fig. 4, A and B). Moreover, treating the lower leaves of wild-type tobacco plants with MeSA induced SAR in the upper, untreated leaves. This required SABP2 in the untreated, but not treated, leaves (Fig. 4, C to E).

SA-deficient rootstocks expressing salicylate hydroxylase (SH) can generate a SAR signal (*4*); therefore, MeSA can act as a mobile signal only if it is not metabolized by SH. Analysis of recombinant SH revealed no activity against MeSA (fig. S2). Moreover, plants expressing SH accumulated MeSA to nearly wild-type levels in primary infected leaves and in systemic leaves, although peak accumulation was delayed ~24 hours (Fig. 3, D and E). MeSA levels in phloem exudates of SH-expressing plants were intermediate between those in wild-type and A13L plants. Because MeSA is synthesized from SA, SA-deficient plants expressing SH might be expected to have very depressed MeSA levels. The similar level of MeSA in SH transgenic and wild-type plants suggests that the kinetic properties of NtSAMT1 and SH are very different, with NtSAMT1 having higher affinity for SA (lower Michaelis-Menten constant K_m) and/or faster kinetics (higher catalytic rate constant k_{cat}) than SH. Alternatively, NtSAMT1 and SH may be in different subcellular locations, with NtSAMT1 having greater (or earlier) access than SH to newly synthesized SA.

A

Mutations	WT	A13L	S81A	H238A
SA binding activity (%)	100	1	~100	0
SA feedback inhibition	+++	–	N/A	N/A
MeSA esterase Activity	+++	+++	–	–
Esterase : SA Binding	E^+B^+	E^+B^-	E^-B^+	E^-B^-

C

Lines	Lesion size (mm ± SD) Primary infection	Secondary infection	% reduction	SAR
Control (C3)	2.49 ± 0.28	0.90 ± 0.15	64	+
SABP2-silenced	2.42 ± 0.37	2.18 ± 0.21	10	–
syn1 SABP2 WT	2.39 ± 0.38	1.08 ± 0.10	55	+
syn1 SABP2 A13L	2.09 ± 0.25	0.43 ± 0.11	79	+
syn1 SABP2 S81A	2.04 ± 0.23	1.58 ± 0.16	22	–
syn1 SABP2 H238A	2.46 ± 0.44	2.08 ± 0.20	16	–
syn2 SABP2 WT	2.30 ± 0.38	0.84 ± 0.08	63	+
syn2 SABP2 A13L	2.50 ± 0.32	0.86 ± 0.12	65	+
syn2 SABP2 S81A	2.66 ± 0.31	2.22 ± 0.22	19	–

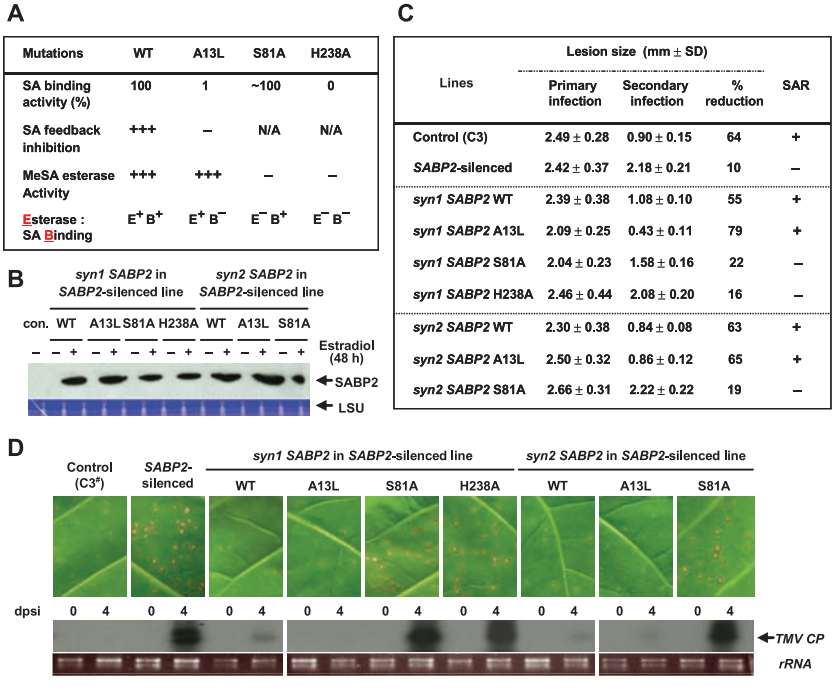

Fig. 2. SABP2's MeSA esterase activity, but not its SA-binding and feedback inhibition activities, is required for SAR in systemic leaves. (**A**) Biochemical characteristics of mutant SABP2 proteins. N/A, not applicable. (**B**) Immunoblot analysis of wild-type or mutant syn SABP2 protein accumulation in 8-week-old stably transformed *SABP2*-silenced tobacco at 0 (–) and 48 hours (+) after treatment with 30 μM estradiol. Expression of endogenous SABP2 was used as a control (con.). The large subunit (LSU) of ribulose bisphosphate carboxylase/oxygenase is shown as a loading control. (**C**) Average lesion size was determined at 5 days post infection (dpi). (**D**) Upper panel: TMV-induced lesions on systemic leaves of plants described in (C) at 5 dpsi. Lower panel: RNA blot analysis of TMV *CP* transcripts in systemic leaves of these plants at 0 and 4 dpsi. For (C) and (D), the transgenes were induced only in systemic leaves (*13*).

The following findings argue that MeSA is a phloem-mobile SAR signal and that SAPB2 is its receptor in systemic tissue: (i) SAR requires SABP2's MeSA esterase activity in the systemic tissue to convert biologically inactive MeSA to active SA (Figs. 1 and 2). (ii) After infection, SA levels rise in the systemic leaves of wild-type plants, whereas little or no rise occurs in SAR-defective, *SABP2*-silenced plants (Fig. 3, F and G). (iii) SAR requires SA-mediated inhibition of this esterase activity in the primary infected leaves (Fig. 3, A and C). (iv) MeSA levels increase after infection in primary infected leaves, and subsequently in phloem exudates of primary infected leaves and in systemic leaves of wild-type plants (Fig. 3, D and E). (v) Reducing MeSA levels in primary infected leaves by expressing the A13L mutant SABP2 with uncontrolled MeSA esterase activity leads to little or no MeSA increase in phloem exudates (Fig. 3E), little or no increase in MeSA and SA in systemic leaves (Fig. 3, D, F, and G), and loss of SAR development (Fig. 3, A to C). (vi) Reducing MeSA levels in primary infected leaves by silencing *NtSAMT1* also results in SAR deficiency (Fig. 4, A and B). (vii) Treating the lower leaves of wild-type tobacco plants with MeSA induces SAR in the upper, untreated leaves. This requires SABP2 in the untreated, but not treated, leaves (Fig. 4, C to E).

MeSA also may be an airborne signal that induces resistance in neighboring plants (*16*). Analyses of the *Arabidopsis dir1-1* and *sfd1* mutants have suggested that the mobile SAR signal is a lipid or lipid derivative (*17*, *18*). Consistent with this possibility, recent studies by Truman *et al.* (*19*) suggest that this lipid-derived signal may be jasmonic acid. It is interesting to note that functional SA analogs induce SAR in both *dir1-1* and *sfd1* mutants (*17*, *18*). Together these studies suggest that a lipid-derived SAR signal works with (or upstream of) MeSA to activate SAR. Thus, there may be two translocated signals that induce SAR: a lipid-derived molecule (perhaps jasmonic acid) and MeSA.

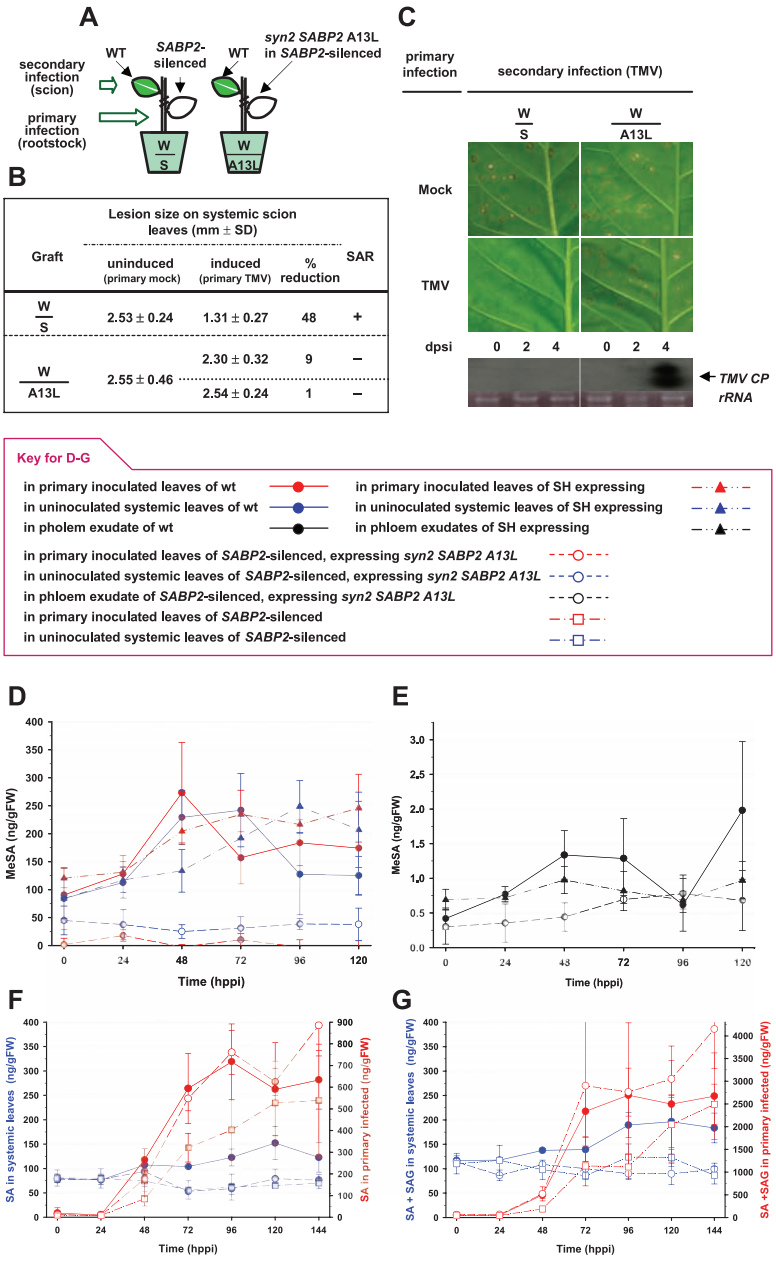

Fig. 3. SAR is compromised by expression of the SABP2 A13L mutant in primary inoculated leaves, and MeSA, SA, and SAG accumulation kinetics after TMV inoculation. (**A**) Schematic of grafting studies using wild-type scions (W, empty vector control) and *SABP2*-silenced (S) rootstocks or *SABP2*-silenced rootstocks expressing the *syn2 SABP2 A13L* transgene (A13L). (**B**) Average lesion size on scion leaves at 5 dpsi. SABP2 A13L synthesis was induced in the rootstocks by estradiol treatment 24 hours before primary inoculation. (**C**) Upper panel: TMV-induced lesions on scion leaves of plants described in (B) at 5 dpsi. Lower panel: analysis of TMV *CP* transcripts in scions at 0, 2, and 4 dpsi. (**D**) MeSA levels in primary inoculated leaves (red) and uninoculated systemic leaves (blue). (**E**) MeSA levels in phloem (petiole) exudates from primary inoculated leaves. (**F** and **G**) SA levels (F) and SA plus SAG levels (G) in primary inoculated leaves (red) and uninoculated systemic leaves (blue). For (D) to (G), the *SABP2 A13L* transgene was induced only in the primary inoculated leaves with estradiol at 24 hours before inoculation. Colors denote measurements in primary leaves (red), secondary leaves (blue), or phloem (black). Solid circles, wild-type plants; open circles, *SABP2*-silenced plants expressing *syn2 SABP2 A13L*; triangles, SA-deficient plants expressing salicylate hydroxylase (SH); squares, *SABP2*-silenced plants.

References and Notes

1. D. Dempsey, J. Shah, D. F. Klessig, *Crit. Rev. Plant Sci.* **18**, 547 (1999).
2. W. E. Durrant, X. Dong, *Annu. Rev. Phytopathol.* **42**, 185 (2004).
3. A. E. Jenns, J. Kuć, *Phytopathology* **69**, 753 (1979).
4. B. Vernooij *et al.*, *Plant Cell* **6**, 959 (1994).
5. J. A. Pallas, N. L. Paiva, C. Lamb, R. A. Dixon, *Plant J.* **10**, 281 (1996).
6. Z. Chen, H. Silva, D. F. Klessig, *Science* **262**, 1883 (1993).
7. D. H. Slaymaker *et al.*, *Proc. Natl. Acad. Sci. U.S.A.* **99**, 11640 (2002).
8. H. Du, D. F. Klessig, *Plant Physiol.* **113**, 1319 (1997).
9. D. Kumar, D. F. Klessig, *Proc. Natl. Acad. Sci. U.S.A.* **100**, 16101 (2003).
10. F. Forouhar *et al.*, *Proc. Natl. Acad. Sci. U.S.A.* **102**, 1773 (2005).
11. M. Seskar, V. Shulaev, I. Raskin, *Plant Physiol.* **116**, 387 (1998).
12. N. Dudareva, R. A. Raguso, J. Wang, J. R. Ross, E. Pichersky, *Plant Physiol.* **116**, 599 (1998).
13. See supporting material on *Science* Online.
14. D. Kumar, C. Gustafsson, D. F. Klessig, *Plant J.* **45**, 863 (2006).
15. J. Zuo, Q.-W. Niu, N.-H. Chua, *Plant J.* **24**, 265 (2000).
16. V. Shulaev, P. Silverman, I. Raskin, *Nature* **385**, 718 (1997).
17. A. M. Maldonado, P. Doerner, R. A. Dixon, C. J. Lamb, R. K. Cameron, *Nature* **419**, 399 (2002).
18. A. Nandi, R. Welti, J. Shah, *Plant Cell* **16**, 465 (2004).
19. W. Truman, M. H. Bennett, I. Kubigsteltig, C. Turnbull, M. Grant, *Proc. Natl. Acad. Sci. U.S.A.* **104**, 1075 (2007).

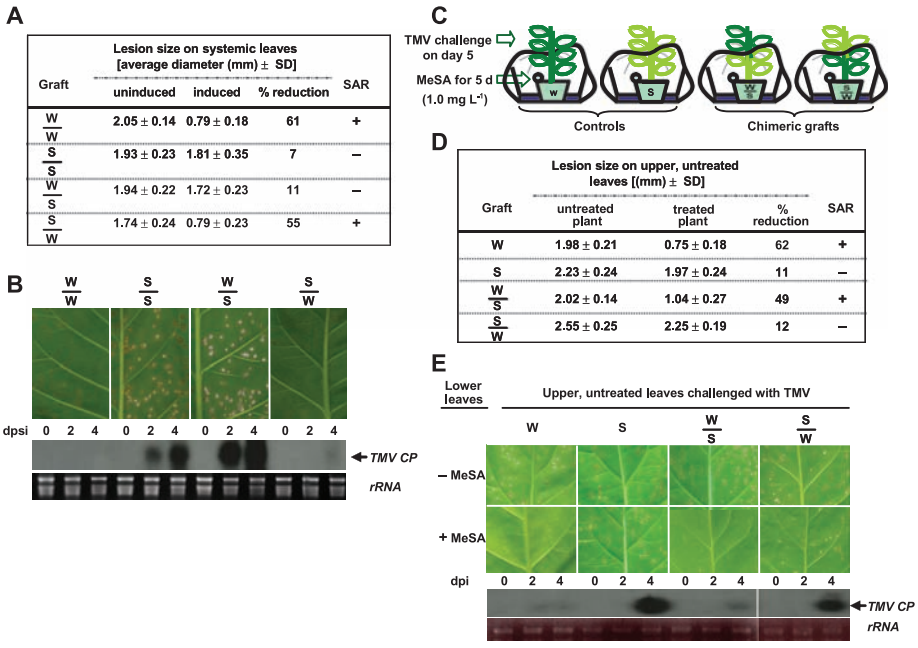

Fig. 4. *NtSAMT1*-silenced tobacco plants are SAR-deficient, and MeSA induces SAR in untreated tissue. (**A**) Determination of lesion size on scions whose rootstocks received either a mock (uninduced) or TMV (induced) inoculation 6 days before a secondary infection with TMV (W, empty vector control; S, *NtSAMT1*-silenced line). (**B**) Upper panel: TMV-induced lesions on scion leaves of the above-described plants at 5 dpsi. Lower panel: RNA blot analysis of TMV *CP* transcripts in scion leaves of these plants at 0, 2, and 4 dpsi. See Fig. 1 legend for details. (**C**) Schematic for MeSA treatment of wild-type (W, empty vector control) and *SABP2*-silenced (S) tobacco. The lower parts of plants (8 weeks old) were treated for 5 days in gas-tight sealed plastic film chambers containing air with or without supplementation with MeSA. After this incubation, the upper, untreated leaves were inoculated with TMV. (**D**) Lesion size on upper, untreated leaves of plants described in (C) at 5 dpi; untreated plants were exposed only to air, whereas treated plants received air supplemented once at the start of the experiment with MeSA (1.0 mg/liter) on the lower leaves. (**E**) Upper panel: TMV-induced lesions on the untreated leaves of plants described in (C) at 5 dpi. Lower panel: RNA blot analysis of TMV *CP* transcripts in untreated leaves at 0, 2, and 4 dpi.

20. We thank L. Tong for advice regarding SABP2 mutational analysis, A. Kessler for advice on GC/MS analyses, N.-H. Chua for estradiol-inducible pER8 vector, DNA2.0 Inc. for synthesizing *syn2 SABP2*, J. Ryals for the transgenic NahG-10 tobacco line encoding a salicylate hydroxylase (*4*), and D. Dempsey for critical comment on the manuscript. Supported by NSF grants IOB-0525360 and DBI-0500550 (D.F.K.).

Supporting Online Material

www.sciencemag.org/cgi/content/full/318/5847/113/DC1
Materials and Methods
Figs. S1 and S2
Table S1
References

27 June 2007; accepted 29 August 2007
10.1126/science.1147113

In Situ Imaging of the Endogenous CD8 T Cell Response to Infection

Kamal M. Khanna, Jeffery T. McNamara, Leo Lefrançois*

Mounting a protective immune response is critically dependent on the orchestrated movement of cells within lymphoid organs. We report here the visualization, using major histocompatability complex class I tetramers, of the CD8-positive (CD8) T cell response in the spleens of mice to *Listeria monocytogenes* infection. A multistage pathway was revealed that included initial activation at the borders of the B and T cell zones followed by cluster formation with antigen-presenting cells leading to CD8 T cell exit to the red pulp via bridging channels. Strikingly, many memory CD8 T cells localized to the B cell zones and, when challenged, underwent rapid migration to the T cell zones where proliferation occurred, followed by egress via bridging channels in parallel with the primary response. Thus, the ability to track endogenous immune responses has uncovered both distinct and overlapping mechanisms and anatomical locations driving primary and secondary immune responses.

An effective immune response depends on the large-scale, but carefully regulated, movement of cells within and between lymphoid and peripheral tissues. In recent years, our understanding of events in secondary lymphoid tissues has been advanced by the use of multiphoton microscopy to visualize lymphocyte movement (*1*–*4*). Nevertheless, much remains to be elucidated about the microanatomy of antigen-specific primary and memory CD8 T cell responses, with relatively limited data currently available from in situ visualization of endogenous CD8 T cell responses (*5*–*7*). Indeed, because of technical difficulties with intravital imaging of the spleen, intravital microscopic analysis of immune responses has been limited to the lymph node and has only elucidated the properties of clonal, single-avidity T cell receptor (TCR) transgenic T cells after transfer of large numbers of cells. Because it is known that increasing naïve T cell precursor frequency affects immune responses (*8*) and that each TCR transgenic T cell exhibits distinct physiological characteristics (*9*), these data should be interpreted with these caveats in mind. Thus, determining the anatomical location and migration of endogenous antigen-specific T cells in lymphoid tissues during primary and secondary immune responses remains an important goal.

To achieve this objective, we used staining with major histocompatability complex (MHC) class I tetramers, which allows in situ identification and localization of clonally diverse endogenous antigen-specific CD8 T cells (*7*). This approach avoids the complications associated with adoptive transfer of TCR transgenic T cells and challenge with model antigens. With this technique, we systematically examined the CD8 T cell response to primary and secondary infection with *Listeria monocytogenes* (LM), which is primarily induced in the spleen (*10*). C57BL/6 mice were infected intravenously with 1×10^6 colony-forming units (CFU) of an attenuated *actA*-deficient strain of LM that had been engineered to express the exogenous antigen ovalbumin

Department of Immunology, University of Connecticut, Farmington, CT 06030, U.S.A.

*To whom correspondence should be addressed. E-mail: Llefranc@neuron.uchc.edu